A Study of Thyratron Control of Tow Phase Servo-Motor

メタデータ	言語: eng 出版者: 公開日: 2010-04-05 キーワード (Ja): キーワード (En): 作成者: Kono, Shigetake, Tokuda, Tsutomu, Hata, Shiro メールアドレス: 所属:
URL	https://doi.org/10.24729/00009111

A Study of Thyratron Control of Tow Phase Servo-Motor

Shigetake KOHNO*, Tsutomu TOKUDA* and Shiro HATA*

(Received February 10, 1958)

Abstract

In general, the two phase induction motor as the servo-motor is controlled through various vacuum tube amplifier or the magnetic amplifiers. In this paper, the analytical and experimental results of the characteristics of thyratron control of two phase induction motor are described.

1. Introduction

At present, the 2-phase induction motor is used in many automatic control fields as the servo-moter, for the reasons of non-commutator, the easy reversibility of turning and the linearity of speed vs. torque characteristics.

Generally, as the control circuit of the 2-phase servo-motor various vacuum tube amplifiers or magnetic amplifiers are adopted. Authers have attempted some analysis and experiment of the thyratron control of a 2-phase induction motor with reduction gear of which ratio is 50:1. In this paper, the results of above analyses and experiments are described.

2. Of the Control of the 2-Phase Induction Moter

As the control method of 2-phase induction motor, there are two methods, one of which is voltage control[1] and the other is phase control[2]. The former is that to the main winding a constant voltage and to the control winding a variable amplitude voltage of which phase differs by 90° from it of main winding are applied respectively. The amplitude of the control winding voltage varies correspondingly to the signal. In this method the stalled torque is proportional to the amplitude of the control winding voltage.

The latter is that to the main and control windings two constants voltage with same amplitude are applied respectively and the phase of the control winding voltage varies for it of the main winding corsespondingly to the signal. In this control the stalled torque is proportional to the sine of the phase difference between two winding voltages.

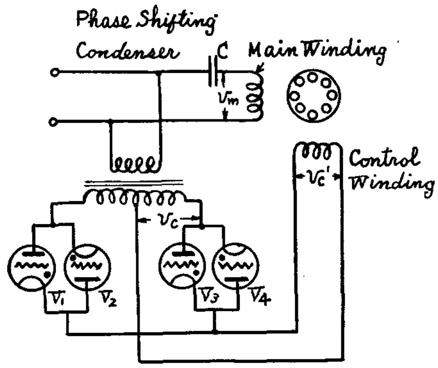

Fig. 1. Thyratron a-c control of 2-phase induction motor.

As shown in Fig. 1 when we control a 2-phase motor by the thyratron directly, the voltage wave form applied to the control winding through the thyratron is shown by the hatched

* Department of Electrical Engineering, College of Enginnering.

portion in Fig. 2, but in where we neglect the thyratron arc voltage and assume that the extinction angle is π rad. This voltage wave form varies with the change of the firing angle θ_f of the thyratron.

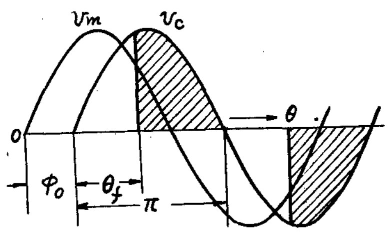

Fig. 2. Voltage wave form in each winding ($\theta_e=\pi$).

Considering only the fundamental component of the such voltage wave form applied to the control winding as shown in Fig. 2, the amplitude and phase of the control winding voltage varies correspondingly to the firing angle θ_f of the thyratron and consequently the motor recieves the above mentioned voltage control and phase control simultaneously.

For the half-wave rectified connection such as case that two thyratron V_2 and V_4 in Fig. 1 are excepted, the previouly described thinking can be also applied.

3. Stalled Torque Produced in the Motor

As shown in Fig. 3, setting $\boldsymbol{V}_m$ and $\boldsymbol{V}_c$ for the vector of the voltage applied to the main and control winding respectively, we can analyze them by the method of symmetrical co-ordinate[1] as follows.

$$\left.\begin{aligned} \boldsymbol{V}_m &= \boldsymbol{V}_{m1}+\boldsymbol{V}_{m2} \\ \boldsymbol{V}_c &= \boldsymbol{V}_{c1}+\boldsymbol{V}_{c2} \\ \boldsymbol{V}_{c1} &= -j\boldsymbol{V}_{m1} \\ \boldsymbol{V}_{c2} &= j\boldsymbol{V}_{m2} \end{aligned}\right\} \quad (1)$$

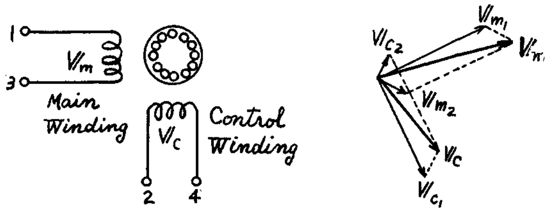

Fig. 3. Vector diagram of each winding voltage and their components analyzed by the method of symmetrical co-ordinate.

positive sequence component;

$$\boldsymbol{V}_{m1} = \frac{\boldsymbol{V}_m + j\boldsymbol{V}_c}{2}$$

negative sequence component;

$$\boldsymbol{V}_{m2} = \frac{\boldsymbol{V}_m - j\boldsymbol{V}_c}{2}\,. \quad (2)$$

Produced torque T in the motor is presented by the sum of the positive and negative sequence torque.

$$T = K_c\{|\boldsymbol{I}_1|^2R_2/s - |\boldsymbol{I}_2|^2R_2/2-s\} = K_d(|\boldsymbol{I}_1|^2/s - |\boldsymbol{I}_2|^2/2-s) \quad (3)$$

where T = produced torque in the motor

s = slip

R_2 = rotor winding resistance

K_c, K_d = constant

$\boldsymbol{I}_1$, $\boldsymbol{I}_2$ = the vector of positive and negative sequence current respectively.

Since $s=1$ at the rest, the stalled troque T_s is given as follows.

$$T_s = K_d(|\boldsymbol{I}_1|^2 - |\boldsymbol{I}_2|^2) = K_d\left(\left|\frac{\boldsymbol{V}_{m1}}{\boldsymbol{Z}_1}\right|^2 - \left|\frac{\boldsymbol{V}_{m2}}{\boldsymbol{Z}_2}\right|^2\right) \tag{4}$$

in where $\boldsymbol{Z}_1$ and $\boldsymbol{Z}_2$ designate the impedance vector of the positive and negative sequence respectively. However, because of $\boldsymbol{Z}_1 = \boldsymbol{Z}_2$ at the rest Eq. (4) becomes

$$T_s = K_e(|\boldsymbol{V}_{m1}|^2 - |\boldsymbol{V}_{m2}|^2)\,. \tag{5}$$

When $\boldsymbol{V}_m$ and $\boldsymbol{V}_c$ are same frequency and their amplitude and phase take each arbitrary value, V_c is presented as follows.

$$\left.\begin{aligned} &\boldsymbol{V}_c = k_1 \boldsymbol{V}_m \cdot \exp\left(-jk_2\frac{\pi}{2}\right). \\ &\text{where} \\ &k_1 = \left|\frac{\boldsymbol{V}_c}{\boldsymbol{V}_m}\right| \\ &k_2 = (\text{Phase difference between } \boldsymbol{V}_m \text{ and } \boldsymbol{V}_c)\Big/\left(\frac{\pi}{2}\right). \end{aligned}\right\} \tag{6}$$

Substituting (6) for $\boldsymbol{V}_c$ in (2), we get $\boldsymbol{V}_{m1}$ and $\boldsymbol{V}_{m2}$, moreover T_s is given.

$$\left.\begin{aligned} \boldsymbol{V}_{m1} &= \frac{\boldsymbol{V}_m}{2}\left[\left\{1 + k_1 \sin\left(k_2\frac{\pi}{2}\right)\right\} + jk_1 \cos\left(k_2\frac{\pi}{2}\right)\right] \\ \boldsymbol{V}_{m2} &= \frac{\boldsymbol{V}_m}{2}\left[\left\{1 - k_1 \sin\left(k_2\frac{\pi}{2}\right)\right\} - jk_1 \cos\left(k_2\frac{\pi}{2}\right)\right] \end{aligned}\right\} \tag{7}$$

$$T_s = T_b \cdot k_1 \sin\left(k_2\frac{\pi}{2}\right) \tag{8}$$

T_b in Eq. (8) desinates the blocked torque produced in the motor when the balanced 2-phase normal voltage is applied. Normalized torque τ is shown as the next.

$$\tau = T_s/T_b = k_1 \sin(k_2\pi/2)\,. \tag{9}$$

When a voltage with an arbitrary amplitude and phase against the main winding voltage is applied to the control winding the produced stalled troque T_s is given from Eq. (6) and (8).

Then, the above described voltage control is the means that k_2 being hold at unity and k_1 is maked to chnge correspondingly to a given control signal, in which case obviously T_s is proportional to the control winding voltage amplitude. The phase control is that k_1 being hold at unity and k_2 varies with a given signal, and T_s is proportional to the sine of the phase difference $(k_2\pi/2)$.

4. A-C Control by the Thyratron

As shown in Fig. 1, when two thyratrons are connected in inverse-parallel and their firing angle θ_f in each half-cycle are equal, the control winding is feeded a-c voltage component only.

Put the main and control winding instanteneous voltage as follows respectively

$$v_m = V_m \sin \omega t \tag{10}$$

$$v_c = V_c \sin(\omega t - \phi_0) \tag{11}$$

moreover

$$V_c = kV_m . \tag{12}$$

When the firing angle in each half-cycle is θ_f, the fundamental component v_c' of the control winding voltage is given by means of Fouier analysis as follows.

$$v_c' = V_c' \sin\{\omega t-(\phi_0+\phi_1)\} \tag{13}$$

where

$$V_c' = \frac{V_c}{\pi}\sqrt{(\pi-\theta_f+\sin\theta_f\cos\theta_f)^2+\sin^4\theta_f} \tag{14}$$

$$\phi_1 = \tan^{-1}\frac{\sin^2\theta_f}{\pi-\theta_f+\sin\theta_f\cos\theta_f} \tag{15}$$

From Eq. (14), (15) and (5)

$$k_1 = \frac{V_c'}{V_m} = \frac{k}{\pi}\sqrt{(\pi-\theta_f+\sin\theta_f\cos\theta_f)^2+\sin^4\theta_f} \tag{16}$$

$$k_2\frac{\pi}{2} = \phi_0+\phi_1=\phi_0+\tan^{-1}\frac{\sin^2\theta_f}{\pi-\theta_f+\sin\theta_f\cos\theta_f} . \tag{17}$$

Substituting (16) and (17) for k_1 and $(k_2\pi/2)$ in (8) respectively, obtained the following relation[3].

$$T_s = T_b\frac{k}{\pi}\{(\pi-\theta_f+\sin\theta_f\cos\theta_f)\sin\phi_0+\sin^2\theta_f\cos\phi_0\} . \tag{18}$$

Using above results, we calculate the relation of θ_f vs. T_s under the condition $k=1$, $\phi_0=\pi/2$ and consequently get the curve (b) in Fig. 4.

The curve (a) in the same Fig. 4 indicates the experimental value under the same condition.

In above analysis we took the assumption that the extinction angle in each half cycle of each thyratron is equal to π rad. However, actually the extinction angle is not π rad, but greater than π rad, because of the existence of inductance in the control winding, and the actual wave form of applied voltage to the control winding is what shown the hatched portion in Fig. 5.

Considering the inductance of the motor winding, let θ_e designates the extinction angle. For the case of $\theta_e>\pi$, we acquire the following relations (19) and (20) which correspond to (14) and (15) respectively, by

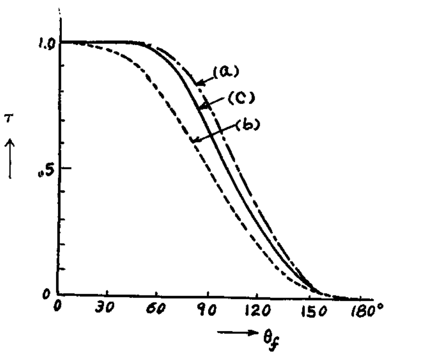

Fig. 4. Normalized torque vs. firing angle characteristics.
(a) Theoretical value ($\theta_e>\pi$).
(b) Theoretical value ($\theta_e=\pi$).
(c) Experimental value.

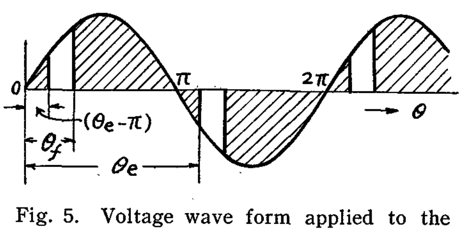

Fig. 5. Voltage wave form applied to the control winding in a-c control ($\theta_e>\pi$).

means of Fourier analysis as same as previously mentioned.

$$V_c' = \frac{V_c}{\pi}\sqrt{\left\{\theta_e-\theta_f+\left(\frac{\sin 2\theta_f-\sin 2\theta_e}{2}\right)\right\}^2+(\sin\theta_e-\sin\theta_f)^2} \tag{19}$$

$$\phi_1 = \tan^{-1}\frac{\sin^2\theta_e-\sin^2\theta_f}{\theta_e-\theta_f+\dfrac{\sin 2\theta_f-\sin 2\theta_e}{2}}. \tag{20}$$

The stalled torque for the case $\theta_e>\pi$ is presented by the following equation within the range $\theta_f\geqq\theta_e-\pi$.

$$T_s = T_b\frac{k}{\pi}\left\{\left(\theta_e-\theta_f+\frac{\sin 2\theta_f-\sin 2\theta_e}{2}\right)\sin\phi_0-(\sin^2\theta_e-\sin^2\theta_f)\cos\phi_0\right\}. \tag{21}$$

Neglecting the arc drop in the thyratron tube following relation exists[4].

$$\sin(\theta_e-\theta) = \sin(\theta_f-\theta)\exp\left(-\frac{\theta_e-\theta_f}{\tan\theta}\right) \tag{22}$$

where θ=power factor angle of the control winding under the blocked condition.

Using the experimental value of θ_e of the motor under test we calculate the relation τ vs. θ_f, and consequently get the curve (c) in Fig. 4 of the case $k=1$ and $\phi_0=\pi/2$. The calculated value shown in the curve (c) roughly coincides with the experimental value shown in the curve (a).

Whthin the range $\theta_f\leqq\theta_e-\pi$, since the control widing being connected always to the source voltage through either tharatron which is conductive, the firing angle is not controlable by this time. That is, within this range T_s holds a constant value in spite of the control of θ_f.

In a-c control, the control winding voltage contains no d-c component, but because of the inverse-parallel connection of two thyratrons there are some inconveniences in the control system such as need to use d-c voltage bias, moreover four tubes are necessary for the reversible operation.

5. Phase Shifting Condenser and Half Wave Control

In Fig. 6 (b), the voltage and current vector diagram of the fundamental component

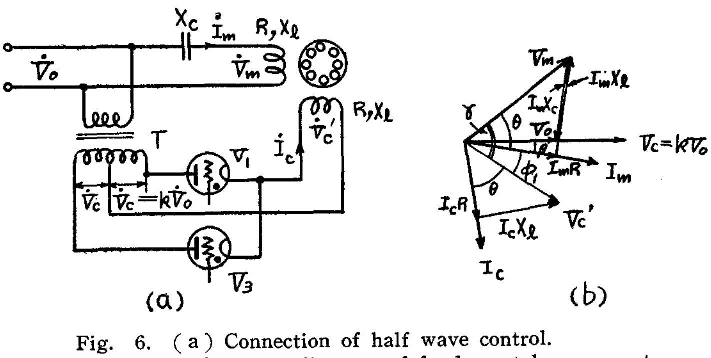

Fig. 6. (a) Connection of half wave control.
(b) Vector diagram of fundamental component at the rotor rest in thyratron control.

at the rotor rests is shown under the thyratron control with a capacitive reactance X_c as phase shifting devise in series to the main winding. R and X_l are the resistance and inductive reactance of each stator winding.

γ designates the phase difference between the main winding voltage and control winding voltage. k_1 is the amplitude ratio of the fundamental component of the control winding voltage to the control winding source voltage and ϕ_1 is their phase difference.

From the vector diagram imediately given the following relations.

$$V_m = \frac{V_0}{\sqrt{R^2+(X_l+X_c)^2}}\sqrt{R^2+X_l^2} \tag{23}$$

$$V_c' = kk'V_0 \tag{24}$$

$$\gamma = k_2\pi/2 = \theta-\beta+\phi_1 \tag{25}$$

$$\sin\beta = \frac{X_l-X_c}{\sqrt{R^2+(X_l-X_c)^2}}. \tag{26}$$

From (23), (24) and (16) result

$$k_1 = \frac{V_c'}{V_m} = kk'\sqrt{\frac{R^2+(X_l-X_c)^2}{R^2+X_l^2}} \tag{27}$$

$$\sin\gamma = \frac{1}{\sqrt{R^2+X_l^2}\sqrt{R^2+(X_l-X_c)^2}}[\{R^2+X_l(X_l-X_c)\}\sin\phi_1+RX_c\cos\phi_1]. \tag{28}$$

Putting

$$X_l/R = Q, \quad X_c = aX_l, \quad (a=\text{const.}) \tag{29}$$

we get the following relation from (8), (27) and (28)

$$T_s = T_bkk'\frac{[\{1+Q^2(1-a)\}\sin\phi_1+aQ_1\cos\phi_1]}{1+Q^2}. \tag{30}$$

From (17) and (25)

$$\phi_0 = \theta-\beta. \tag{31}$$

Since $\phi_1=0$ when $\theta_f=0$, the relation between a and Q which satisfies the condition $\phi_0=\pi/2$, is acquired.

That is,

$$a = \frac{1+Q^2}{Q^2}. \tag{32}$$

Substituting (32) for a in (30) results

$$T_s = T_bkk'\frac{1}{Q}\cos\phi_1. \tag{33}$$

Using (29) and (32) the necessary phase shifting condenser is determined.

As described in previous section, the thyratron a-c control has some inconveniences. But the simple half wave control circuit as shown in Fig. 6 (a) is available too. In this control, neglecting arc drop in the thyratron, the control winding

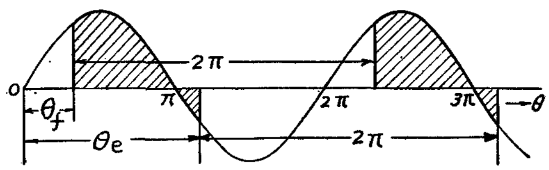

Fig. 7. Voltage wave form applied to the control winding in half wave control.

wave form is given by the calculated value $k' \cos \phi_1$ of the motor under test is presented by the curve (b) in Fig. 8. The other curve (a), (c) and (d) show experimental characteristics of τ vs. θ_f. The curve (a) was obtained when $V_m = V_c = 100$ volts, (c) when $V_m = 100$ volts, $V_c = 140$ volts, (d) when $V_m = V_c = 100$ volts and the control windings shunted by a phanotron in inverse polarity.

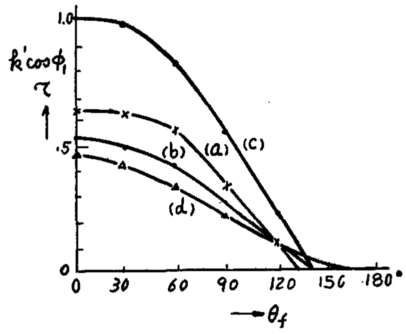

Fig. 8. Normalized torque vs. firing angle characteristics in half wave control.

The half wave rectified control has a few merit compared with the thyratron a-c control, that is, this control method needs a simple grid control circuit, and half number of thyratron. Moreover containg d-c component, the damping character is improved.

The curve (c) in Fig. 8 shows that in the half wave rectified control the same output is obtainable as a-c control produces by the adoption of suitable value for k.

6. Conclusion

The analytical and experimental results of the stalled torque in the induction motor under the thyratron control are described above.

As above mentioned, in the thyratron control, there are two methods, one of which, the half wave rectified control is favourable in the point of the simplisity and the damping characteristics.

References

1) For Example, A. E. Fitzgerald: "Electric Machinary" (1952).
2) A. Steinhaker, E. Meserve: T.A.I.E.E **70** (1951).
3) S. Kohno, T. Tokuda, S. Hata: in Annual Meeting of I.E.E of Japan, Nagoya, April (1955).
4) K. Miyakoshi, S. Hata, Y. Kojima: J.I.E.E of Japan **75**. 134 (1955).